JHEP

Published for SISSA by Springer

Received: April 29, 2016
Revised: August 8, 2016
Accepted: September 25, 2016
Published: October 14, 2016

Large-N $\mathbb{C}P^{N-1}$ sigma model on a finite interval

Stefano Bolognesi,[a,b] **Kenichi Konishi**[a,b] **and Keisuke Ohashi**[a,b,c]

[a] *Department of Physics "E. Fermi", University of Pisa, Largo Pontecorvo, 3, Ed. C, 56127 Pisa, Italy*

[b] *INFN — Sezione di Pisa, Largo Pontecorvo, 3, Ed. C, 56127 Pisa, Italy*

[c] *Osaka City University Advanced Mathematical Institute, 3-3-138 Sugimoto, Sumiyoshi-ku, Osaka 558-8585, Japan*

E-mail: stefanobolo@gmail.com, kenichi.konishi@unipi.it, keisuke084@gmail.com

Abstract: We analyze the two-dimensional $\mathbb{C}P^{N-1}$ sigma model defined on a finite space interval L, with various boundary conditions, in the large N limit. With the Dirichlet boundary condition at the both ends, we show that the system has a unique phase, which smoothly approaches in the large L limit the standard $2D$ $\mathbb{C}P^{N-1}$ sigma model in confinement phase, with a constant mass generated for the n_i fields. We study the full functional saddle-point equations for finite L, and solve them numerically. The latter reduces to the well-known gap equation in the large L limit. It is found that the solution satisfies actually both the Dirichlet and Neumann conditions.

Keywords: 1/N Expansion, Sigma Models, Solitons Monopoles and Instantons

ArXiv ePrint: 1604.05630

doi:10.1007/JHEP10(2016)073

JHEP10(2016)073

Contents

1 Introduction **1**

2 $\mathbb{C}P^{N-1}$ sigma model on a finite space interval **2**
- 2.1 Generalized gap equations 3
- 2.2 Translational invariance Ansatz 5

3 Solution of the generalized gap equation **7**
- 3.1 Behavior of the functions $\lambda(x)$ and $\sigma(x)$ near the boundaries 8
- 3.2 Numerical solutions for $\lambda(x)$ and $\sigma(x)$ 11
- 3.3 Absence of the "Higgs" phase 15

4 Discussion **15**

A Eigenfunctions near the boundaries **16**

JHEP10(2016)073

1 Introduction

The non linear $\mathbb{C}P^{N-1}$ sigma model in two dimensions has been extensively studied in the past starting from the works [1, 2]. It has many properties in common with QCD in four dimensions, such as asymptotic freedom, mass gap, confinement and the existence of a topological sector. Moreover it has the advantage of being solvable in the large-N limit. Recently the $\mathbb{C}P^{N-1}$ sigma model appeared in the study of low energy effective action on certain topological solitons such as the non-Abelian string [3–5].

In this paper we study the large-N solution of the bosonic $\mathbb{C}P^{N-1}$ model on a finite interval of length L with various types of boundary conditions. The periodic boundary condition has been previously studied as a thermal compactification in [6, 7] and more recently in [8]. One key feature for the solvability of this model is that the periodic compactification preserves translational invariance.

The problem with the Dirichlet boundary condition in a finite interval has been studied recently in [9] by using a translational invariance Ansatz, where two possible phases were found: a confinement phase with mass generation at large L and a Higgs phase for a shorter string $L < L_{\rm crit} \sim 1/\Lambda$.

It is the purpose of the present paper to examine in depth the bosonic $\mathbb{C}P^{N-1}$ model on a finite-width strip, with Dirichlet or Neumann conditions at the space boundaries. The exact functional saddle-point equations will be studied in the large N limit, with no a priori assumption about the translational invariance. It will be seen that while with the periodic boundary condition the translational invariance Ansatz is indeed consistent with the full set of equations of motion, the generalized gap equations cannot be satisfied by a

translational invariant (constant) mass-generation Ansatz when the D-D or N-N boundary condition is used. The solution which satisfies the full set of equations is found numerically, for various values of L.

Contrary to a claim made in [9] we find that the system has a unique phase, which smoothly approaches the "confinement phase" in the large L limit. The physical reason for this result may be found in the fact that, for small L, the system reduces in the infrared (the large wavelength) limit effectively to a one-dimensional (quantum mechanics) system where we do not expect to find any phase transitions.

2 $\mathbb{C}P^{N-1}$ sigma model on a finite space interval

The classical action for the $\mathbb{C}P^{N-1}$ sigma model is given by

$$S = \int dxdt \left((D_\mu n_i)^* D^\mu n_i - \lambda (n_i^* n_i - r) \right) , \tag{2.1}$$

where n^i with $i = 1, \ldots, N$ are N complex scalar fields and the covariant derivative is $D_\mu = \partial_\mu - iA_\mu$. Configurations related by a U(1) gauge transformation $z_i \to e^{i\alpha} z_i$ are equivalent: the U(1) gauge field A_μ does not have a kinetic term in the classical action. λ is a Lagrange multiplier that enforces the classical condition

$$n_i^* n_i = r , \tag{2.2}$$

where r is the "size" of the $\mathbb{C}P^{N-1}$ manifold, which is the radius of S^2 sphere for $N = 2$, and can also be expressed in terms of the coupling constant by

$$r = \frac{4\pi}{g^2} . \tag{2.3}$$

Since n appears only quadratically in the Lagrangian, it can be integrated out in the partition function

$$Z = \int [dA_\mu][d\lambda][dn_i][dn_i^*]\, e^{iS} = \int [dA_\mu][d\lambda]\, e^{iS_{\text{eff}}} , \tag{2.4}$$

thus leaving an effective action for A_μ and λ:

$$S_{\text{eff}} = \int d^2x \left(N \,\text{tr}\log(-D_\mu^* D^\mu + \lambda) - \lambda r \right) . \tag{2.5}$$

The condition of stationarity with respect to λ leads to the gap equation which is conveniently written in the Euclidean formulation as

$$r - N \,\text{tr} \left(\frac{1}{-\partial_\tau^2 - \partial_x^2 + m^2} \right) = 0 , \tag{2.6}$$

where we have set $A_\mu = 0$ and $\lambda = m^2$. An expectation value of λ provides a mass for the n_i particles (here we assumed a constant vacuum expectation value for λ; see however below). On the infinite line the spectrum is continuous and the gap equation reads

$$r = N \int_0^{\Lambda_{\text{UV}}} \frac{kdk}{2\pi} \frac{1}{k^2 + m^2} = \frac{N}{4\pi} \log \left(\frac{\Lambda_{\text{UV}}^2 + m^2}{m^2} \right) , \tag{2.7}$$

JHEP10(2016)073

leading to the well-known scale-dependent renormalized coupling

$$r(\mu) = \frac{4\pi}{g(\mu)^2} \simeq \frac{N}{2\pi} \log\left(\frac{\mu}{\Lambda}\right) \tag{2.8}$$

and to a dynamically generated mass, which in the case of the infinite line can be taken to coincide with the dynamical scale Λ,

$$m = \Lambda \, . \tag{2.9}$$

2.1 Generalized gap equations

The $\mathbb{C}P^{N-1}$ theory on a finite interval of length L, $0 < x < L$ will now be considered. For this problem the boundary conditions must be specified. One possibility is the Dirichlet boundary condition which, up to a U(N) transformation, is the following constraint on the boundary

$$\text{D-D}: \qquad n_1(0) = n_1(L) = \sqrt{r} \, , \qquad n_i(0) = n_i(L) = 0 \, , \quad i > 1 \, . \tag{2.10}$$

For simplicity and for definiteness, we take in this paper the n_i field in the same direction in the $\mathbb{C}P^{N-1}$ space at the two boundaries. Another possibility is the Neumann boundary condition

$$\text{N-N}: \qquad \partial_x n_i(0) = \partial_x n_i(L) = 0 \, . \tag{2.11}$$

We consider in detail the three possible combinations D-D, N-N and periodic boundary conditions. More possibilities are open for the choice of classical boundary condition but, for reasons to be clarified later, there is no need to list all of them.

The N fields can be separated into a classical component $\sigma \equiv n_1$ and the rest, n^i ($i = 2, \ldots, N$). Integrating over the $N-1$ remaining fields yields the following effective action

$$S_{\text{eff}} = \int d^2x \left((N-1) \, \text{tr} \log(-D_\mu D^\mu + \lambda) + (D_\mu \sigma)^* D^\mu \sigma - \lambda(|\sigma|^2 - r) \right) \, . \tag{2.12}$$

One can take σ real and set the gauge field to zero, and consider the leading contribution at large N only. The total energy can formally be written as

$$E = N \sum_n \omega_n + \int_0^L \left((\partial_x \sigma)^2 + \lambda(\sigma^2 - r) \right) dx \, , \tag{2.13}$$

where ω_n^2 are the eigenvalues of the following operator

$$\left(-\partial_x^2 + \lambda(x) \right) f_n(x) = \omega_n^2 \, f_n(x) \, , \tag{2.14}$$

and f_n are the corresponding eigenfunctions. The eigenfunctions f_n can be taken to be real and orthonormal

$$\int_0^L dx \, f_n(x) f_m(x) = \delta_{n\,m} \, . \tag{2.15}$$

JHEP10(2016)073

The expression for the energy (2.13) is not regularized yet, it still contains quadratic, linear and logarithmic divergences with the UV cutoff. For the moment we shall work with this formally divergent expression for the energy. The eigenfunctions f_n's satisfy also the completeness condition

$$\sum_{n=1}^{\infty} f_n(x) f_n(x') = \sum_{n\in Z} \Big(\delta(x - x' + 2\,nL) \mp \delta(x + x' + 2\,nL) \Big) \,, \tag{2.16}$$

where $\mp$ refers respectively to the Dirichlet or Neuman conditions. Note that for $x, x' \in [0, L]$, only the first term $\delta(x - x')$ is relevant; other terms guarantee that the completeness condition is consistent with the boundary condition (the mirror image method).

The two functions $\sigma(x)$ and $\lambda(x)$ must be determined by extremizing the energy (2.13). Varying the action with respect to $\sigma(x)$ one gets

$$\partial_x^2 \sigma(x) - \lambda(x)\sigma(x) = 0 \,. \tag{2.17}$$

In a translationally invariant system (i.e. with constant λ and σ) this equation reduces to $\lambda\,\sigma = 0$. This implies that either one of the condensates λ or σ must vanish. It follows that there are in general two possible distinct phases which are generally called "confinement phase" ($\lambda \neq 0$, $\sigma = 0$) or "Higgs phase" ($\lambda = 0$, $\sigma \neq 0$). In a non-translational invariant system there is no net distinction between these two phases since in general both $\lambda(x)$ and $\sigma(x)$ are different from zero.

The variation of the spectrum of the operator (2.14) for $\lambda(x) \to \lambda(x) + \delta\lambda(x)$ is given by

$$\delta\omega_n^2 = \int_0^L dx\, \delta\lambda(x) f_n(x)^2 \,, \tag{2.18}$$

to first order in $\delta\lambda(x)$, as can be seen easily from (2.14). The variation of the energy (2.13) with respect to $\lambda(x)$ then gives

$$\frac{N}{2} \sum_n \frac{f_n(x)^2}{\omega_n} + \sigma(x)^2 - r = 0 \,. \tag{2.19}$$

We find it convenient to separate this equation into a constant part (the average in x) plus a non-constant part with zero integral. First write σ^2 as

$$\sigma^2 = \widetilde{\sigma}^2 + \frac{1}{L}\int_0^L \sigma^2 dx \,, \qquad \int_0^L \widetilde{\sigma}^2 dx = 0 \,. \tag{2.20}$$

eq. (2.19) can thus be separated into the one for the constant part

$$\frac{N}{2L} \sum_n \frac{1}{\omega_n} + \frac{1}{L}\int_0^L \sigma^2 dx - r = 0 \,, \tag{2.21}$$

and another for the non-constant part

$$\frac{N}{2} \sum_n \frac{1}{\omega_n} \left(f_n(x)^2 - \frac{1}{L} \right) + \widetilde{\sigma}^2 = 0 \,. \tag{2.22}$$

JHEP10(2016)073

So the three equations to be solved for $\lambda(x)$ and $\sigma(x)$ are (2.17), (2.21) and (2.22). Only eq. (2.21) needs to be regularized since it contains a logarithmic divergence with the UV cutoff.

For later use we provide a relation between the expression $\sum_n \frac{f_n(x)^2}{\omega_n}$ that appears in the generalized gap equation and the Euclidean propagator. The Euclidean propagator satisfies

$$\left(-\frac{\partial^2}{\partial\tau^2}-\frac{\partial^2}{\partial x^2}+\lambda(x)\right)D(x,\tau;x',\tau') = \\ = \delta(\tau-\tau')\sum_{n\in Z}\Big(\delta(x-x'+2\,nL)\mp\delta(x+x'+2\,nL)\Big) \tag{2.23}$$

and, in terms of $\{f_n,\omega_n\}$, it is given by

$$D(x,\tau;x',\tau')\equiv\sum_n\frac{e^{-|\tau-\tau'|\omega_n}}{2\omega_n}f_n(x)f_n(x')\ . \tag{2.24}$$

We can thus infer the useful relation

$$\sum_n\frac{f_n(x)^2}{2\omega_n}=\lim_{\epsilon\to 0}D(x,\epsilon;x,0)\ , \tag{2.25}$$

where the Euclidean time interval ϵ plays the role of the UV cutoff. At this stage it is easy to see that the generalized gap equation (2.19) is nothing but a quantized version of the defining condition (2.2):

$$\big\langle n_i(x)^* n^i(x)\big\rangle - r\equiv\sigma(x)^2+\lim_{\epsilon\to 0}(ND(x,\epsilon,x,0))-r=0\ . \tag{2.26}$$

2.2 Translational invariance Ansatz

Let us first test if the Ansatz of a translationally invariant (constant) λ is consistent with our functional saddle-point equations. Let us consider first the D-D case. If $\lambda=m^2$ were constant the eigenfunctions and eigenvalues of the operator (2.14) would be simply given by

$$f_n(x)=\sqrt{\frac{2}{L}}\sin\left(\frac{n\pi x}{L}\right),\qquad \omega_n=\sqrt{\left(\frac{n\pi}{L}\right)^2+m^2}\ ,\qquad n\geq 1,\quad n\in\mathbb{Z}\ . \tag{2.27}$$

Here one has an explicit representation of the propagator,

$$D(x,\tau;x',\tau') = \sum_{n\in Z}\frac{1}{2\pi}K_0(m\sqrt{(x-x'+2nL)^2+(\tau-\tau')^2}) \\ -\sum_{n\in Z}\frac{1}{2\pi}K_0(m\sqrt{(x+x'+2nL)^2+(\tau-\tau')^2})\ . \tag{2.28}$$

Note that each term satisfies the standard Green function equation (2.23) with a single delta function in x on the right hand side. In the case with a constant σ, eq. (2.21) gives,

JHEP10(2016)073

by using an appropriate regularization

$$
\begin{aligned}
0 &= \frac{N}{2L}\sum_n \frac{1}{\omega_n} + \sigma^2 - r \\
&= \lim_{\epsilon\to 0}\frac{1}{L}\int_0^L dx\,(ND(x,\epsilon;x,0) - r) + \sigma^2 \\
&= \frac{N}{2\pi}\ln\frac{\Lambda}{m} - \frac{N}{4mL} + \frac{N}{\pi}\sum_{n=1}^{\infty} K_0(2nmL) + \sigma^2
\end{aligned}
\tag{2.29}
$$

which is nothing but the gap equation discussed by Milekhin [9]. Here, taking into account the consistency with eq. (2.9) for infinite string, the dynamical scale Λ can be introduced as

$$
r = \frac{4\pi}{g^2} = \frac{N}{2\pi}\left(\ln\frac{2}{\Lambda\epsilon} - \gamma\right) \quad \leftrightarrow \quad \Lambda = \frac{2}{\epsilon}\exp\left(-\frac{8\pi^2}{Ng^2} - \gamma\right) \tag{2.30}
$$

where γ is the Euler-Mascheroni constant. The second term in the last line of eq. (2.29) comes from the infinite mirror poles:

$$
\frac{N}{2\pi}\frac{1}{L}\sum_{n\in Z}\int_0^L dx K_0(2m|x+nL|) = \frac{N}{2\pi}\frac{1}{L}\int_{-\infty}^{\infty} dx\, K_0(2m|x|) = \frac{N}{4mL}\,. \tag{2.31}
$$

One can verify that eq. (2.29) gives the local extremum (maximum) of the total energy (2.13)

$$
E = \frac{Nm^2L}{2\pi}\left(\frac{1}{2} - \log\frac{m}{\Lambda}\right) - \frac{Nm}{2} - \frac{Nm^2L}{\pi}\sum_{n=1}^{\infty}\frac{K_1(2\,n\,m\,L)}{n\,mL} + m^2L\sigma^2 \tag{2.32}
$$

with respect to m^2, under the translational-invariance Ansatz.

However, the problem is that an additional equation, (2.22), must be satisfied as well. The left hand side, using $\widetilde{\sigma} = 0$ (under the assumption of translational invariance), is just

$$
\frac{N}{2L}\sum_{n=1}^{\infty}\frac{1}{\omega_n}\left(2\sin^2\left(\frac{n\pi x}{L}\right) - 1\right) = -\frac{N}{2L}\sum_{n=1}^{\infty}\frac{1}{\omega_n}\cos\left(\frac{2n\pi x}{L}\right)\,, \tag{2.33}
$$

which is equal to, by using (2.25),

$$
\begin{aligned}
N\lim_{\epsilon\to 0}&\left(D(x,\epsilon;x;0) - \frac{1}{L}\int_0^L dx D(x,\epsilon;x;0)\right) \\
&= \frac{N}{2L}\left(\frac{1}{2m} - \frac{L}{\pi}\sum_{n\in\mathbb{Z}} K_0(2m|x-nL|)\right).
\end{aligned}
\tag{2.34}
$$

This is clearly not zero: eq. (2.22) is not satisfied by a constant m.

For N-N boundary conditions and $\lambda = m^2$ constant the eigenmodes are

$$
f_n(x) = \sqrt{\frac{2}{L}}\cos\left(\frac{n\pi x}{L}\right), \quad \omega_n = \sqrt{\left(\frac{n\pi}{L}\right)^2 + m^2}\,, \qquad n \geq 0\,, \quad n\in\mathbb{Z} \tag{2.35}
$$

JHEP10(2016)073

In this case, the left hand side of eq. (2.22) gives

$$\frac{N}{2L}\sum_{n=0}^{\infty}\frac{1}{\omega_n}\left(2\cos^2\left(\frac{n\pi x}{L}\right)-1\right)=\frac{N}{2L}\sum_{n=1}^{\infty}\frac{1}{\omega_n}\cos\left(\frac{2n\pi x}{L}\right)$$
$$=-\frac{N}{2L}\left(\frac{1}{2m}-\frac{L}{\pi}\sum_{n\in\mathbb{Z}}K_0(2m|x-nL|)\right). \quad (2.36)$$

which is the same as the D-D case (2.33), except for the sign. The proof is as before by using instead the plus sign in (2.23). Again, eq. (2.22) cannot be satisfied by a constant λ.

Thus both for DD and NN boundary conditions, the constant generated mass m does not represent a quantum saddle point of our system.

For the periodic boundary condition one can set for convenience the period length to $2L$. The complete set of eigenstates and eigenfunctions are exactly given by a D-D set (2.27) plus a N-N set, (2.35), applied in the enlarged space $[0, 2L]$. In this case, the left hand side of equation (2.22) is the sum of D-D states contribution (2.33) plus the N-N states contribution (2.36) which cancel. As expected, the translational invariance Ansatz is consistent in this case. This system has been studied in [8]. With a periodic condition, the total energy and the gap equation can depend on the Wilson loop $\exp(i\int_0^{2L}A_x dx)$. With a nonvanishing constant gauge field A_x, one finds that the propagator is given by

$$D(x,\tau;x',\tau')=\sum_{n\in Z}\frac{1}{2\pi}K_0(m\sqrt{(x-x'+2nL)^2+(\tau-\tau')^2})\,e^{iA_x(x-x'+2nL)}. \quad (2.37)$$

Therefore the energy in the confinement phase ($\sigma=0$), is [8]

$$E=\frac{Nm^2L}{\pi}\left(\frac{1}{2}-\log\frac{m}{\Lambda}\right)-\frac{2Nm^2L}{\pi}\sum_{n=1}^{\infty}\frac{K_1(2n\,mL)}{n\,mL}\cos(2nA_xL). \quad (2.38)$$

By minimizing the energy with respect to A_x, one finds $A_x=0$. The saddle point with respect to m^2 is determined by the gap equation

$$0=\frac{N}{2\pi}\ln\frac{\Lambda}{m}+\frac{N}{\pi}\sum_{n=1}^{\infty}K_0(2nmL). \quad (2.39)$$

In this case no other equations must be satisfied, so this gives the solution of the problem.

3 Solution of the generalized gap equation

Having proven that a constant $\lambda=m^2$ does not satisfy the functional saddle point equations, (2.17), (2.21) and (2.22), for the problem with the Dirichlet or Neumann boundary conditions, we now discuss the solution of these equations, relying also on a numerical analysis. The content of this section constitutes the main new contribution of this paper.

3.1 Behavior of the functions $\lambda(x)$ and $\sigma(x)$ near the boundaries

Before embarking on the numerical analysis one must first understand the behavior close to the boundaries of the two unknown functions $\lambda(x)$ and $\sigma(x)$. For the case of D-D boundary condition, and under the assumption of constant λ, the left hand side of (2.22) is given by (2.33) and thus contains a logarithmic divergence near the boundaries since $K_0(x) \simeq -\log x$ for $x \ll 1$. In the propagator formalism (2.34) this leading divergence comes from the closest mirror pole. The logarithmic behavior is due to the fact that at $x \ll 1$ one can neglect the potential λ and use the massless propagator. Another crude, but somehow useful, way to understand this logarithm divergence is the following. At fixed x, we split the sum (2.33) into "low-energy" modes and "high-energy" modes. For the low-energy modes we approximate $\sin^2\left(\frac{n\pi x}{L}\right) \simeq 0$. The high-energy modes instead are summed to zero due to the fast averaging. The result gives the correct log divergent term:

$$\frac{N}{2L}\sum_{n=1}^{[L/\pi x]}\frac{1}{\omega_n}\left(2\sin^2\left(\frac{n\pi x}{L}\right)-1\right)+\frac{N}{2L}\sum_{n=[L/\pi x]+1}^{\infty}\frac{1}{\omega_n}\left(2\sin^2\left(\frac{n\pi x}{L}\right)-1\right)$$
$$\simeq \frac{N}{2L}\sum_{n=1}^{[L/\pi x]}\frac{1}{\omega_n}(-1) \simeq \frac{N}{2\pi}\log x + \dots \ . \tag{3.1}$$

We will show below more carefully that this type of divergence near the boundary is really there, at least for the D-D condition, also for a generic, but not too singular, potential $\lambda(x)$. Let us use the WKB approximation to compute the leading divergence of $\sum_n \frac{f_n(x)^2}{\omega_n}$ near the boundaries of the interval. We assume $\lambda(x)$ to be generic, with $\lambda(x) > 0$ and $\lambda(x) = \lambda(L-x)$, but not too singular near the boundaries:

$$\lim_{x\to 0} x^2\lambda(x) = 0 \ . \tag{3.2}$$

It will be seen that the potential $\lambda(x)$ is non-constant and divergent near the boundaries $\lambda(x) \to \infty$ as $x \to 0, L$. Nevertheless it does satisfy the condition (3.2). This fact also implies that 'the Higgs phase' defined by a configulation in which the potential vanishes identically, $\lambda(x) = 0$, cannot be a solution of the generalized gap equation. By using WKB approximation the high-energy modes of the operator (2.14) can be approximated, in the classically allowed region, by

$$f_n(x) \simeq \frac{C_n}{\sqrt{p_n(x)}}\sin\left(\int_{\epsilon_n}^{x} p_n(x')dx' - \frac{\theta_n}{2}\right) \tag{3.3}$$

where

$$p_n(x) = \sqrt{\omega_n^2 - \lambda(x)}, \qquad C_n = \sqrt{\frac{2}{\int_{\epsilon_n}^{L-\epsilon_n}\frac{dx}{p_n(x)}}} \tag{3.4}$$

and ϵ_n and $L-\epsilon_n$ are the classical turning point

$$\omega_n^2 - \lambda(\epsilon_n) = 0 \ , \qquad \omega_n^2 - \lambda(L-\epsilon_n) = 0 \ . \tag{3.5}$$

JHEP10(2016)073

The Bohr-Sommerfeld quantization condition is

$$\int_{\epsilon_n}^{L-\epsilon_n} \sqrt{\omega_n^2 - \lambda(x)}\, dx = \pi\, n + \theta_n \,, \qquad n \in \mathbb{Z}_{>0} \,. \tag{3.6}$$

The initial phase θ_n is quite important to determine the divergence near the boundaries. It would be equal to $\pi/2$ if there were no boundary, but a smooth classical turning point. However, the phase θ_n turns out to vanish

$$\theta_n = 0 \,, \tag{3.7}$$

as can be seen as follows. If $\lambda(x)$ had the maximum λ_M, then for $\omega_n > \sqrt{\lambda_M}$ there was no classical turning point and the classically allowed region was $[0, L]$ ($\epsilon_n = 0$) and we get $\theta_n = 0$ due to the D-D condition. Even in the case where λ diverges at the boundaries, which actually is our case, the same result is obtained because, from the condition (3.2) and the equation (3.5), one gets

$$\lim_{\omega_n \to \infty} \omega_n\, \epsilon_n = 0 \,, \tag{3.8}$$

meaning that the turning point ϵ_n goes to zero faster than the typical wave length of the eigenstate, $\sim 1/\omega_n$. This is sufficient for letting us to conclude that for large n the eigenfunctions and eigenvalues are well approximated by

$$f_n \simeq \sqrt{\frac{2}{L}} \sin\left(\frac{n\pi x}{L}\right) \,, \qquad \omega_n \simeq \frac{n\pi}{L} \,, \tag{3.9}$$

and thus

$$\frac{N}{2} \sum_n \frac{1}{\omega_n} \left(f_n(x)^2 - \frac{1}{L} \right) \simeq -\frac{N}{2\pi} \sum_{n=1}^{\infty} \frac{1}{n} \cos\left(\frac{2n\pi x}{L}\right) = \frac{N}{2\pi} \log\left(2 \sin\left(\frac{\pi x}{L}\right)\right) \,, \tag{3.10}$$

which behaves indeed near $x = 0$ as

$$\sim \frac{N}{2\pi} \log x \,. \tag{3.11}$$

In other words, the sum of the fluctuations of the n_i fields very generally produces a divergent behavior for the first two terms of eq. (2.22) near the boundaries, quite independently of the form of $\lambda(x)$, as long as the latter satisfies the condition (3.2). The only way to solve eq. (2.22) is then to cancel this divergence with the classical field σ

$$\sigma^2 \simeq \frac{N}{2\pi} \log \frac{1}{x} \,. \tag{3.12}$$

But this is exactly the expected behavior, as it corresponds to the classical constraint (2.2), or to the D-D boundary condition, (2.10), as can be seen once a renormalized coupling (2.8) with energy scale $\mu = 1/x$ is substituted. Approaching the boundaries, $x \sim \epsilon, L - \epsilon$, is thus similar to going into the UV, hence the classical value for $\sigma(x) = n_1(x)$ there (see more on this point below).

JHEP10(2016)073

The divergence of the σ field near the boundaries (3.12) on the other hand implies, through equation (2.17), that the potential λ also diverges. Its leading behavior at $x \simeq 0$ is given by

$$\lambda(x) \simeq \frac{1}{2\,x^2 \log 1/x} \tag{3.13}$$

which indeed satisfies the condition, (3.2).

Thus the behavior of the functions $\lambda(x)$ and $\sigma(x)$ near the boundaries has been determined self-consistently to be given by (3.12) and (3.13) (and similarly for $x \sim L$, with $x \to L - x$).

Physically, such a behavior can be understood as follows. At any fixed x, far from the boundaries, the UV divergences due to the higher modes are cancelled by a constant (and divergent) $r_\epsilon = \frac{4\pi}{g_\epsilon^2}$, exactly as in the standard $\mathbb{C}P^{N-1}$ sigma model without the space boundaries. This is so because the UV divergences are local effects in x: far from the boundaries the effects of the latter are negligible. Near the boundaries where the quantum fluctuations of the n_i fields are suppressed, however, this cancellation cannot occur, r_ϵ being a constant. This is where the classical field $\sigma = n_1$ comes to rescue. The generalized gap equation (2.19) is now satisfied by balancing the "ultraviolet" divergent behavior of $\sigma(x)$ at $x \sim \epsilon$, with r_ϵ.

Even though this way of interpreting (3.12) and (3.13) is straightforward in the case of the D-D condition, actually the same results hold for the system with the N-N boundary condition as well. They just tell that at the boundaries, where the quantum fluctuations of the n_i fields are suppressed and cannot produce the logarithmic divergences due to the lack of the two-dimensional spacetime, the defining condition (2.26) of the $\mathbb{C}P^{N-1}$ theory must be satisfied by the classical field,[1] independently of the type of the boundary condition. The numerical solutions found below indeed hold true both for the case of the D-D and the N-N boundary conditions.

This conclusion can be further confirmed by studying the wave functions $f_n(x)$ analytically near the boundaries, assuming $\lambda(x)$ of the form of (3.13), as is done in appendix A. The resulting behavior is

$$f_n(x \to 0) \propto \frac{x}{\sqrt{-\log x}}\,; \qquad f_n(x \to L) \propto \frac{L-x}{\sqrt{-\log\,(L-x)}}\,. \tag{3.14}$$

Thus not only do they satisfy the Dirichlet boundary condition but also the Neumann boundary condition. As already anticipated, this is the indication one gets from the numerical solution found by the recursive procedure to be described in the next subsection. The results found for $\lambda(x)$ and $\sigma(x)$ turn out to be the same, irrespectively of the boundary condition used to solve the wave equation (2.14).

Finally we note that the case of the periodic boundary condition is qualitatively different. In that case, the points $x = 0, L$ are no special points, the quantum fluctuations are effective there, as well as at any other point, and our results (3.12) and (3.13) do not apply. Such system has been recently studied in [8].

[1] Note that in the large N approximation we are working in, "quantum fluctuations" of the σ field are suppressed by $1/N$ as compared to those of n_i, $i \neq 1$, as well as to its classical mode.

JHEP10(2016)073

3.2 Numerical solutions for $\lambda(x)$ and $\sigma(x)$

The method we employ to solve the set of equations (2.17), (2.21), and (2.22) numerically is as follows. We first introduce a finite cutoff $n_{\max}$ on the number of modes. Accordingly, equation (2.21) can be regularized as (see eq. (2.8)) [2]

$$\frac{N}{2L}\sum_{n=1}^{n_{\max}}\frac{1}{\omega_n}+\frac{1}{L}\int_0^L\sigma^2 dx-\frac{N}{2\pi}\log\left(\frac{2\mu(n_{\max})}{\Lambda}\right)=0\,, \tag{3.17}$$

where, by using (3.9),

$$\mu(n_{\max})=\frac{n_{\max}\pi}{L}\,. \tag{3.18}$$

The algorithm we use here to find the solution, somewhat reminiscent of Hartree's equations in atomic physics, is a recursive procedure in which at each step k one has a certain function $\lambda_k(x)$, with some initial $\lambda_0(x)$ satisfying (3.13). Given $\lambda_k(x)$, the Schrödinger equation (2.14) is solved to give $\{\omega_n, f_n(x)\}$ for the desired number of modes; (2.22) and (3.17) are then used to find the corresponding value of σ_k^2:

$$\sigma_k^2=-\frac{N}{2}\sum_n\frac{1}{\omega_n}\left(f_{n,k}(x)^2-\frac{1}{L}\right)-\frac{N}{2L}\sum_{n=1}^{n_{\max}}\frac{1}{\omega_{n,k}}+\frac{N}{2\pi}\log\left(\frac{2\mu(n_{\max})}{\Lambda}\right)\,. \tag{3.19}$$

Note that the right hand side of this equation depends only on $\lambda_k(x)$.

The next iteration for λ is found by use of eq. (2.17):

$$\lambda_{k+1}(x)=\frac{\partial_x^2\sigma_k(x)}{\sigma_k(x)}\,. \tag{3.20}$$

This procedure can be repeated until a convergence to a consistent set of $\lambda(x)$ and $\sigma(x)$ is achieved[3]. We set L fixed and then study various values of Λ. We take the starting point of the iteration to be $\lambda_0(x)=0$ for the first value of Λ. For the successive values of Λ, the self-consistent solution $\lambda(x)$ obtained with the previous value of Λ will be taken as the starting point $\lambda_0(x)$ of recursion.

The method as described above works well for $L\Lambda$ up to 1 after which it loses convergence. The delicate point in the algorithm is the step (3.20) which is exceedingly sensitive

[2] A careful change of the regularization gives the factor 2 in front of $\mu(n_{\max})$ so that it is consistent with eq. (2.9). Omitting higher modes larger than $n_{\max}$

$$\frac{\pi}{L}\sum_{n=n_{\max}+1}^{\infty}\frac{e^{-\epsilon\omega_n}}{\omega_n}\simeq\sum_{n=n_{\max}+1}^{\infty}\frac{e^{-\frac{n\pi}{L}\epsilon}}{n}\simeq-\log(1-e^{-\frac{\pi}{L}\epsilon})-\sum_{n=1}^{n_{\max}}\frac{1}{n}\simeq-\log\epsilon-\log\mu(n_{\max})-\gamma\,, \tag{3.15}$$

introduces a translation between the two UV cut-off parameters ϵ and $\mu(n_{\max})$ as $1/\epsilon=\mu e^{\gamma}$. Therefore, eq. (2.30) giving Λ is translated as

$$r=\frac{N}{2\pi}\left(\log\frac{2}{\Lambda\epsilon}-\gamma\right)=\frac{N}{2\pi}\log\frac{2\mu(n_{\max})}{\Lambda}\,. \tag{3.16}$$

[3] The whole analysis has been performed by using Mathematica, Wolfram (Version 10.3). The spectra $\{f_n, \omega_n\}$ at each recursion step are found by use of the command "NDEigensystem".

JHEP10(2016)073

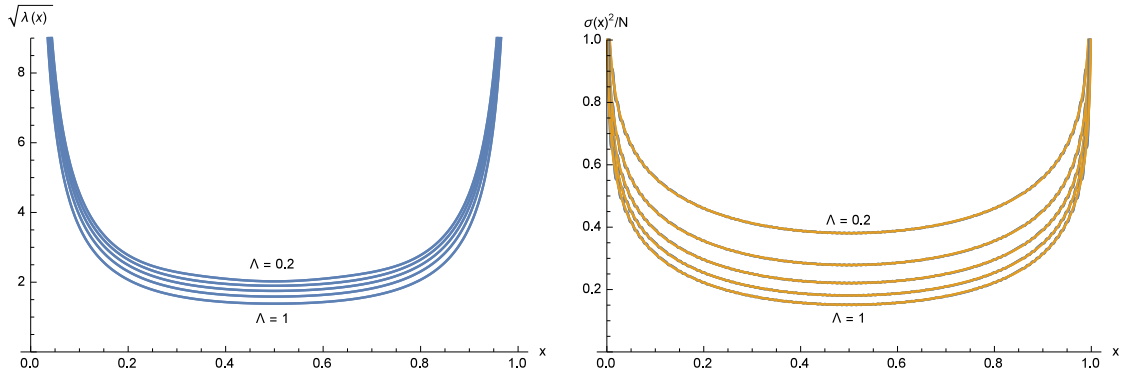

Figure 1. On the left $\sqrt{\lambda(x)}$, on the right $\sigma(x)^2/N$. These plots are obtained by keeping $L = 1$ fixed and changing Λ.

to small variations of $\sigma_k(x)$ in the denominator. A technical improvement we implement is the following. We substitute (3.20) with a "smoother" recursive formula

$$\lambda_{k+1}(x) = \frac{1}{K}\left(\frac{\partial_x^2\sigma_k(x)}{\sigma_k(x)} + (K-1)\lambda_k(x)\right) , \tag{3.21}$$

with some conveniently chosen K. Having a larger value of K makes the convergence slower but at the same time it allows to reach higher values of $L\Lambda$. For example by choosing $K = 15$ (as is done to produce the plots for large $L\Lambda$ given below) one can reach $L\Lambda$ up to 4.

Another technical issue is that $\sigma_k(x)$, as computed in (3.19), cannot be inserted as it is in the second derivative of the expression for $\lambda_{k+1}(x)$. In passing from (3.19) to (3.21) one must perform a numerical fit to approximate $\sigma_k(x)$ with a sum of analytical functions. In the plots given below $\sigma_k(x)$ and its analytical fit are superimposed: the two curves are indistinguishable, within the resolution of the graphs.

Results. In figure 1 we present some numerical results for smaller values of $L\Lambda$. $\sqrt{\lambda(x)}$ is shown in the left panel while the right panel gives the classical field $\sigma(x)^2/N$. The figures show the results for $L = 1$ fixed and $\Lambda = 0.2, 0.4, 0.6, 0.8, 1$.

Figure 2 shows the plots for fixed dynamical scale $\Lambda = 1$ and various values of L. The results in the two figures are related by a trivial rescaling. The only non-trivial dimensionless quantity is ΛL. Two cases with the same ΛL are related by the following scale transformation

$$\frac{1}{\alpha^2}\lambda\left(\frac{x}{\alpha};\frac{L}{\alpha},\Lambda\alpha\right) = \lambda(x;L,\Lambda) ; \qquad \sigma\left(\frac{x}{\alpha};\frac{L}{\alpha},\Lambda\alpha\right) = \sigma(x;L,\Lambda) . \tag{3.22}$$

Another visualization of the results is given in figure 3 where the value of the fields at the center of the string, $L/2$, is shown for various values of L and at fixed $\Lambda = 1$.

The results for larger values of $L\Lambda$ are shown in figure 4, for $\Lambda = 1$ fixed and $L = 1, 2, 3, 4$. From the figures we see the expected pattern emerging: by going to larger L at fixed Λ one expects to recover the confined phase of the standard $\mathbb{C}P^{N-1}$ sigma model,

JHEP10(2016)073

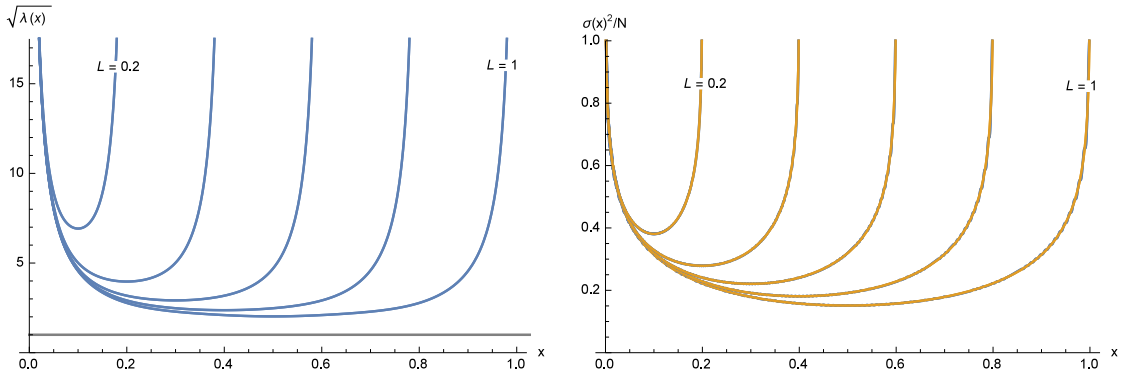

Figure 2. On the left $\sqrt{\lambda(x)}$, on the right $\sigma(x)^2/N$. These plots are the corresponding of figure 1 but rescaled in order to keep $\Lambda = 1$ fixed and changing L. The constant line on the left figure is Λ.

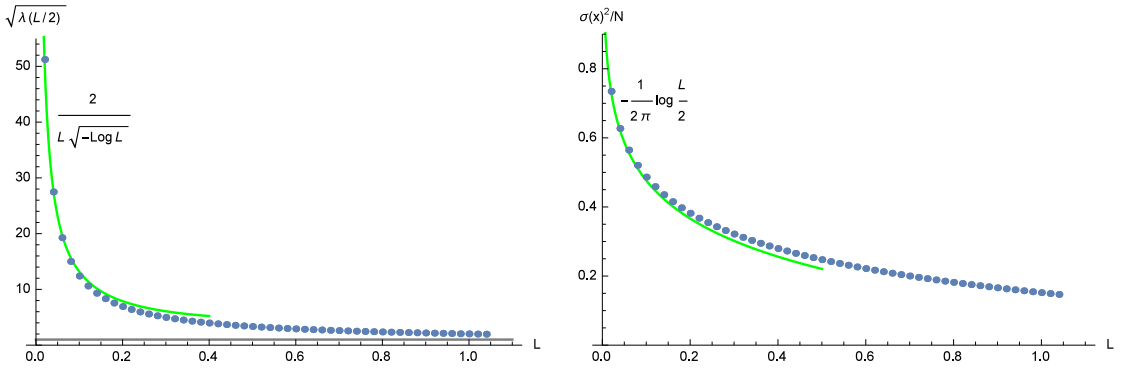

Figure 3. On the left is $\sqrt{\lambda(L/2)}$; on the right $\sigma(L/2)^2/N$ for various values of L keeping $\Lambda = 1$. The data points are compared with the singular behavior (3.12) and (3.13) extrapolated towards the center of the string, $L/2$.

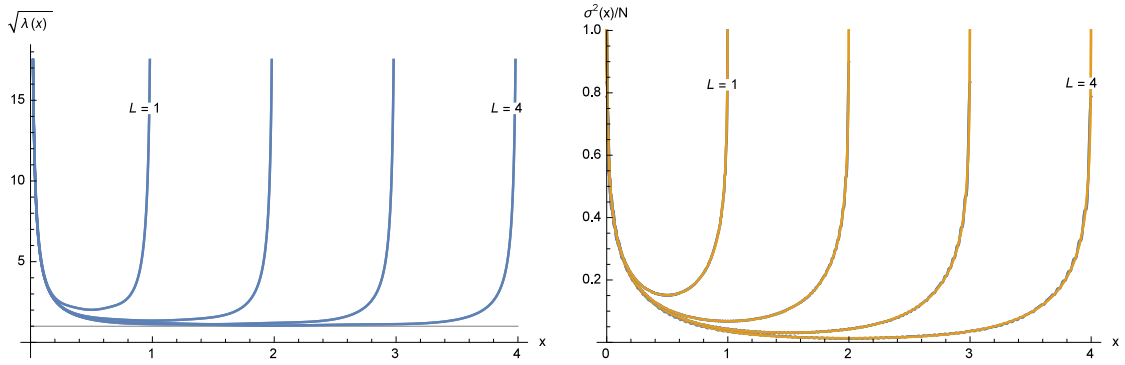

Figure 4. On the left $\sqrt{\lambda(x)}$, on the right $\sigma(x)^2/N$. These plots are rescaled in order to keep $\Lambda = 1$ fixed and for $L = 1, 2, 3, 4$. The constant line on the left figure is Λ.

JHEP10(2016)073

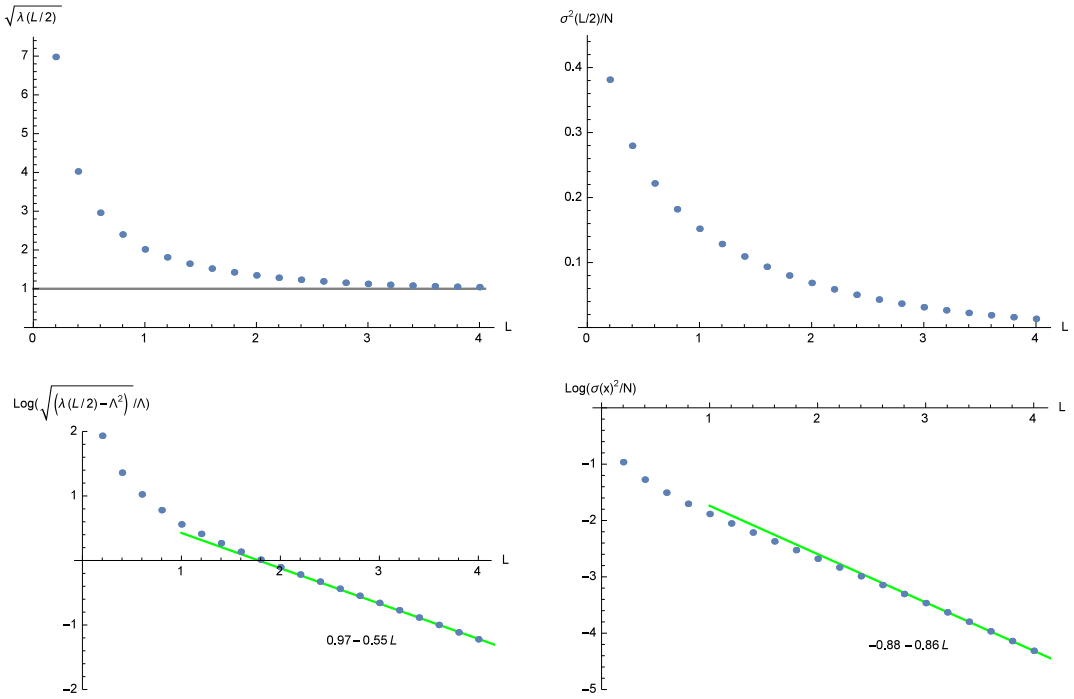

Figure 5. These plots are: on the top-left is $\sqrt{\lambda(L/2)}$, on the top-right $\sigma(L/2)^2/N$, on the bottom-left $\log\left(\sqrt{\lambda(L/2)-\Lambda^2}/\Lambda\right)$ and on the bottom-right $\log\left(\sigma^2(L/2)/N\right)$. These plots are obtained for various values of L keeping $\Lambda = 1$.

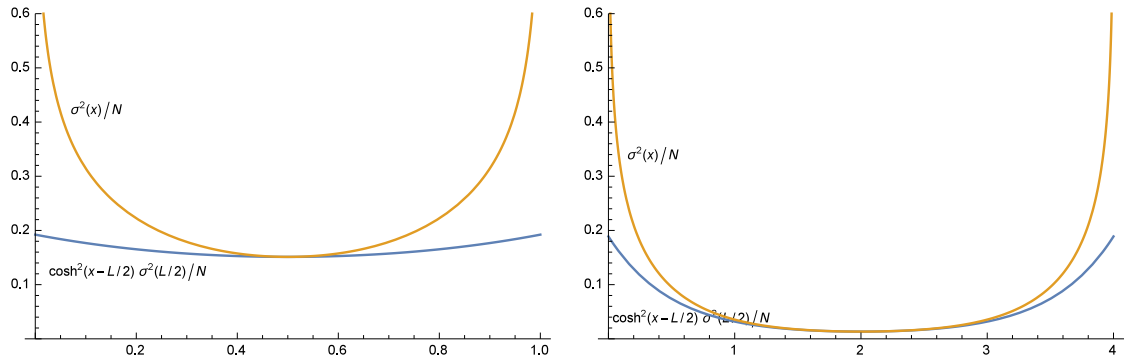

Figure 6. $\sigma(x)^2/N$ compared with the *cosh* approximation for $\Lambda = 1$ and $L = 1$ on the left and $L = 4$ on the right.

eq. (2.9). We indeed see that $\sqrt{\lambda(x)} \to \Lambda$ in the middle of the interval whereas the condensate σ approaches zero there at the same time. The effects of the boundary remain concentrated near the two extremes and do not propagate beyond $1/\Lambda$.

The values of the fields at the middle point of the interval are given in figure 5 where in the bottom line are the corresponding logarithmic plots to show better the rate of convergence to the confinement phase. A linear fit to the logarithmic plots at large L, both

JHEP10(2016)073

for $\log\left(\sqrt{\lambda(L/2)-\Lambda^2}/\Lambda\right)$ and for $\log\left(\sigma^2(L/2)/N\right)$, or

$$\lambda\left(\frac{L}{2}\right) \simeq \Lambda^2 + \Lambda^2 e^{0.97-0.55L}\,; \qquad \sigma\left(\frac{L}{2}\right)^2 \simeq N\, e^{-0.88-0.86L}\,, \tag{3.23}$$

is a fairly clear signal that the boundary effects are exponentially suppressed at fixed x, for large values of L.

As a further check of our conclusion, figure 6 shows that the field $\sigma(x)$ becomes indeed well approximated by a hyperbolic cosine function in the central region for large L. As seen from eq. (2.17) this is what is to be expected for $\sigma(x)$, upon dynamical generation of the mass for n_i, $\langle\lambda\rangle = \Lambda^2$.

3.3 Absence of the "Higgs" phase

The preceding analysis clearly shows that the solution of the set of the generalized gap equations is unique: it smoothly approaches in the large L limit the well-known physics of the $\mathbb{C}P^{N-1}$ model (at large N) in "confinement phase" with

$$\langle\sigma(x)\rangle = 0\,; \qquad \langle\lambda(x)\rangle = m^2 = \Lambda^2\,, \tag{3.24}$$

(see figures 1–5). It is however really a simple matter to prove directly the absence of the "Higgs phase", characterized by the condensates

$$\langle\sigma(x)\rangle = \text{const.} \sim \Lambda\,, \quad \langle\lambda(x)\rangle = 0 \tag{3.25}$$

for any value of L. The proof is basically identical to the proof already given (subsection 2.2) of the fact that translationally invariant condensates, λ and σ constant, are not consistent with the generalized gap equations: rather, it is a special case of it. Indeed, if the n field mass is not generated, $\lambda \equiv 0$, the approximation used for higher levels ($n \gg 1$) (see eq. (3.9), eq. (3.10)) is actually valid for all levels. Thus one finds that the first term of the gap equation (2.22) is given exactly by,

$$\frac{N}{2}\sum_n \frac{1}{\omega_n}\left(f_n(x)^2 - \frac{1}{L}\right) = \frac{N}{2\pi}\log\left(2\sin\left(\frac{\pi x}{L}\right)\right)\,, \tag{3.26}$$

which is certainly not equal to 0 identically. This proves that the Higgs phase is not possible in the presence of the boundaries, except for the case with the periodic boundary conditions.

4 Discussion

In this paper we have studied in detail the two-dimensional $\mathbb{C}P^{N-1}$ model with a finite space interval. In other words the system is defined on a finite-width worldstrip, in which the fields propagate. We find that the system has a unique phase which smoothly approaches in the large L limit the standard $2D$ $\mathbb{C}P^{N-1}$ system in confinement phase, with (constant) mass generation for the n_i fields, which are then confined by a $2D$ Coulomb force.

JHEP10(2016)073

This kind of model is of great interest in physics. For instance, it appears as the low-energy effective theory describing the quantum excitations of monopole-vortex soliton complex [10–13]. In such a context, the $\mathbb{C}P^{N-1}$ model describes the nonAbelian orientational zeromodes of the nonAbelian vortex (string), whereas its boundaries represent the monopoles arising from a higher-scale gauge-symmetry breaking, carrying the same orientational $\mathbb{C}P^{N-1}$ moduli. NonAbelian monopoles, which are not plagued by the well-known pathologies, emerge in such a context, and the infrared properties of such a soliton complex is an important question, defining the dynamical properties of the nonAbelian monopoles.

As the $\mathbb{C}P^{N-1}$ sigma model in two dimensions is asymptotically free, i.e., it is a theory which is scale invariant in the UV, one might wonder what the meaning of the "finite interval" L is. The point is that the behavior of the system in the UV — where the effects of the space boundaries should be negligible — contains in itself by dimensional transmutation the renormalization-invariant mass scale Λ (equivalent to specifying the value of the coupling constant at the ultraviolet cutoff, Λ_{UV}), whether or not the system dynamically flows actually into the infrared regime at $1/\Lambda$ where the interactions become strong. The space interval L can be defined in reference to $1/\Lambda$.

But this implies that for $L \ll 1/\Lambda$ quantum fluctuations would not become strongly coupled, their wavelengths constrained to be smaller than $1/\Lambda$. In other words, the system effectively reduces to a finite dimensional object propagating in time, i.e., quantum mechanics, rather than a proper $2D$ quantum field theory. This would explain our finding that the $\mathbb{C}P^{N-1}$ model with a space boundary has a unique phase.

With the periodic boundary condition, the story could be different. The translational invariance is unbroken, and it could be a property of the vacuum: the constant mass $\lambda(x) = m^2$ (or σ) generation of the order of Λ is certainly consistent with the functional saddle-point equations, as we have shown. Even $L < 1/\Lambda$ the system thus maintains $2D$ field-theoretic properties, and it could be [8] that, at large N, the system shows a phase transition at a critical length $L_{crit} = O(1/\Lambda)$, from confinement ($m \sim \Lambda$, $\sigma = 0$) to Higgs ($\sigma \sim \Lambda, m = 0$) phase.

Acknowledgments

We thank Alessandro Betti and Simone Giacomelli for discussions, Ettore Vicari for useful comments, and Gerald Dunne for communications. The work of SB is funded by the grant "Rientro dei Cervelli Rita Levi Montalcini" of the Italian government. The present research work is supported by the INFN special research project grant, GAST ("Gauge and String Theories").

A Eigenfunctions near the boundaries

$\lambda(x)$ satisfying the generalized gap equation was found to behave as

$$\lambda(x) \approx -\frac{1}{2x^2 \log x} \approx \frac{\Lambda_0^2}{2} e^{\frac{2}{y}} y \,, \tag{A.1}$$

JHEP10(2016)073

around $x = 0$, where

$$y = y(x) \equiv \frac{1}{-\log(\Lambda_0 x)} , \qquad x = \Lambda_0^{-1} e^{-1/y} , \tag{A.2}$$

and Λ_0 is some constant. In terms of the new coordinate y, $\tilde{\lambda}(y) \equiv \lambda(x)$ has an essential singularity at $y = 0$. It is natural to assume that $\lambda(x)$ can be expanded around the boundary at $x = 0\,(y = 0)$ as

$$\lambda(x) = \tilde{\lambda}(y) = \Lambda_0^2 \sum_{n=0}^{\infty} e^{-\frac{n-2}{y}} v_n(y) , \tag{A.3}$$

where $v_n(y)$ are functions with no essential singularities. Especially, we set for $v_0(y)$

$$v_0(y) = \frac{y}{2} + \sum_{n=2}^{\infty} a_n y^n . \tag{A.4}$$

The $n = 0$ term in (A.3) gives the dominant contribution since

$$\lim_{y \to +0} \frac{e^{-\frac{n-1}{y}} v_{n+1}(y)}{e^{-\frac{n-2}{y}} v_n(y)} = 0 . \tag{A.5}$$

Note that the knowledge of an exact form of $v_0(y)$ and poles of $v_1(y)$ is needed to determine the divergent contribution to the following integral

$$r \int_{\epsilon}^{L-\epsilon} \lambda(x) dx \approx 2r \int_{\epsilon} \left(\frac{v_0(y(x))}{x^2} + \frac{v_1(y(x))}{x} \right) dx = \frac{N}{2\pi\epsilon} + \mathcal{O}\left(-\frac{1}{\epsilon \log \epsilon} \right) \tag{A.6}$$

and to renormalize the total energy. An incomplete knowledge of the subdominant divergences in $\lambda(x)$ and $\sigma(x)$ for the moment prevents us from removing these divergences from the energy unambiguously. We expect that these divergences are independent of the length L; the resulting finite contribution may be interpreted as the mass of the endpoints (the monopole mass).

Given the potential $\lambda(x)$, the behavior of an eigenfunction $f(x)$ near the boundaries can be inferred directly from

$$\left(-\partial_x^2 + \lambda(x) \right) f(x) = \omega^2 f(x) , \tag{A.7}$$

where we dropped the level number, as the leading behavior near $x = 0$ or $x = L$ turns out to be independent of the energy level. We assume an expansion of the form

$$f(x) = \sum_{n=0}^{\infty} e^{-\frac{n+\rho}{y}} h_n(y) , \qquad h_n(y) = \sum_{k=0}^{\infty} c_{n,k}\, y^{k+\delta_n} . \tag{A.8}$$

for $f(x)$, with constants ρ, δ_n. Substituting (A.3) and (A.8) into eq. (A.7) one sees that the dominant terms on the left hand side are of the order of $O(e^{\frac{2-\rho}{y}})$, whereas the right

hand side is $O(e^{\frac{-\rho}{y}})$, which is smaller by $e^{-2/y} \sim x^2$. Requiring thus that the leading $e^{\frac{2-\rho}{y}}$ terms of eq. (A.7) to vanish, one is led to the following equation

$$y^4 h_0''(y) + y^2(2y + 2\rho - 1)h_0'(y) + (\rho(\rho - 1) - v_0(y))h_0(y) = 0 \,. \tag{A.9}$$

By inserting the expansion (A.8) for $h_0(y)$, this can be solved recursively for $c_{0,k}$:

$$\begin{aligned} \rho(\rho-1)\, c_{0,k+2} + \left((k+\delta_0+1)(2\rho-1) - \frac{1}{2}\right) c_{0,k+1} \\ = (a_2 - (k+\delta_0)(k+\delta_0+1))\, c_{0,k} + \sum_{m=1}^{\infty} a_{m+2}\, c_{0,k-m} \,. \end{aligned} \tag{A.10}$$

As $c_{0,k} = 0$ $(k < 0)$, these recursion relations require

$$(\rho, \delta_0) = \left(0, -\frac{1}{2}\right), \quad \text{or} \qquad \left(1, \frac{1}{2}\right) \,, \tag{A.11}$$

that is,

$$f(x) \sim \sqrt{-\log x}\,, \qquad \text{or} \qquad \frac{x}{\sqrt{-\log x}} \,, \tag{A.12}$$

near $x = 0$. Actually the above recursive relations define two different solutions of the equation (A.9) for $h_0(y)$.

Similarly, by considering terms of the order of $\exp \frac{-n+2-\rho}{y}$, one finds a recursive relation for $h_n(y)$ which has a *unique* solution, *given* $\{h_0(y), h_1(y), \cdots, h_{n-1}(y), \omega\}$.

This way one finds the general solution of eq. (A.7):

$$f(x) = A_1 f_\omega^{(1)}(x) + A_2 f_\omega^{(2)}(x) \,, \tag{A.13}$$

where $f^{(1,2)}(x)$ behave around the boundary at $x = 0$ as

$$f_\omega^{(1)}(x) \approx \sqrt{-\log x}\,, \qquad f_\omega^{(2)}(x) \approx \frac{x}{\sqrt{-\log x}} \,. \tag{A.14}$$

As $f_\omega^{(1)}(x), f_\omega^{(2)}(x)$ yield a nonvanishing Wronskian

$$\lim_{x\to 0}(f_\omega^{(1)}(x) f_\omega^{(2)\prime}(x) - f_\omega^{(1)\prime}(x) f_\omega^{(2)}(x)) = 1 \,, \tag{A.15}$$

they clearly represent two linearly independent solutions for given ω.

Our boundary condition requires that the functions $f_n(x)$ describing the quantum fluctuations of the n_i fields choose

$$f_n(x) \propto f_\omega^{(2)}(x) \approx \frac{x}{\sqrt{-\log x}} \,, \tag{A.16}$$

which is the result reported in (3.14). On the other hand, the classical field σ, corresponding to the zero $(\omega = 0)$ mode, was found to opt for (see eq. (3.12))

$$\sigma = \sqrt{\frac{N}{2\pi}} f_\omega^{(1)}(x) \approx \sqrt{\frac{N}{2\pi}} \sqrt{-\log x} \,. \tag{A.17}$$

JHEP10(2016)073

References

[1] A. D'Adda, M. Lüscher and P. Di Vecchia, *A $1/n$ expandable series of nonlinear σ-models with instantons*, *Nucl. Phys.* **B 146** (1978) 63 [INSPIRE].

[2] E. Witten, *Instantons, the quark model and the $1/n$ expansion*, *Nucl. Phys.* **B 149** (1979) 285 [INSPIRE].

[3] A. Hanany and D. Tong, *Vortices, instantons and branes*, *JHEP* **07** (2003) 037 [hep-th/0306150] [INSPIRE].

[4] R. Auzzi, S. Bolognesi, J. Evslin, K. Konishi and A. Yung, *Non-Abelian superconductors: vortices and confinement in $N = 2$ SQCD*, *Nucl. Phys.* **B 673** (2003) 187 [hep-th/0307287] [INSPIRE].

[5] M. Shifman and A. Yung, *Non-Abelian string junctions as confined monopoles*, *Phys. Rev.* **D 70** (2004) 045004 [hep-th/0403149] [INSPIRE].

[6] I. Affleck, *The role of instantons in scale invariant gauge theories*, *Nucl. Phys.* **B 162** (1980) 461 [INSPIRE].

[7] A. Actor, *Temperature dependence of the $\mathbb{C}P^{n-1}$ model and the analogy with quantum chromodynamics*, *Fortsch. Phys.* **33** (1985) 333 [INSPIRE].

[8] S. Monin, M. Shifman and A. Yung, *Non-Abelian string of a finite length*, *Phys. Rev.* **D 92** (2015) 025011 [arXiv:1505.07797] [INSPIRE].

[9] A. Milekhin, *$\mathbb{C}P(N-1)$ model on finite interval in the large-N limit*, *Phys. Rev.* **D 86** (2012) 105002 [arXiv:1207.0417] [INSPIRE].

[10] R. Auzzi, S. Bolognesi, J. Evslin and K. Konishi, *Non-Abelian monopoles and the vortices that confine them*, *Nucl. Phys.* **B 686** (2004) 119 [hep-th/0312233] [INSPIRE].

[11] K. Konishi, A. Michelini and K. Ohashi, *Monopole-vortex complex in a theta vacuum*, *Phys. Rev.* **D 82** (2010) 125028 [arXiv:1009.2042] [INSPIRE].

[12] M. Cipriani, D. Dorigoni, S.B. Gudnason, K. Konishi and A. Michelini, *Non-Abelian monopole-vortex complex*, *Phys. Rev.* **D 84** (2011) 045024 [arXiv:1106.4214] [INSPIRE].

[13] C. Chatterjee and K. Konishi, *Monopole-vortex complex at large distances and nonAbelian duality*, *JHEP* **09** (2014) 039 [arXiv:1406.5639] [INSPIRE].

JHEP10(2016)073